[Prion 1:2, 144-153; April/May/June 2007]; ©2007 Landes Bioscience

Research Paper

Protein Aggregation and Polyasparagine-Mediated Cellular Toxicity in *Saccharomyces cerevisiae*

Theodore W. Peters

Mingxia Huang*

Department of Biochemistry and Molecular Genetics; University of Colorado Health Sciences Center; Aurora, Colorado USA

*Correspondence to: Department of Biochemistry and Molecular Genetics; University of Colorado Health Sciences Center; Mail Stop 8101; P.O. Box 6511; Aurora, Colorado 80045 USA; Tel.: 303.724.3204; Fax: 303.724.3215; Email: mingxia.huang@uchsc.edu

Original manuscript submitted: 05/23/07
Revised manuscript submitted: 06/26/07
Manuscript accepted: 06/26/07

This manuscript was previously published online as a *Prion* E-publication: http://www.landesbioscience.com/journals/prion/article/4630

KEY WORDS

polyasparagine, polyglutamine, protein aggregation, HSP104, RNQ1

ACKNOWLEDGEMENTS

We would like to thank Chris Link (University of Colorado at Boulder) and Min Lu (Weill Cornell Medical College) for critical reading of the manuscript and Pamela Wolfe (UCHSC Colorado Biostatistics Consortium) for assistance with statistical analysis.

ABSTRACT

It is well established that protein aggregation is associated with many neurodegenerative disorders including polyglutamine diseases, but a mechanistic understanding of the role of protein aggregates in the disease pathogenesis remains elusive. Previously thought to be the cause of cellular toxicity such as cellular dysfunction and cell death, protein aggregation is now proposed to serve a protective role by sequestering toxic oligomers from interfering with essential physiological processes. To investigate the relationship between protein aggregation and cellular toxicity, we have characterized and compared the effects of two GFP-fusion proteins that form aggregates in *Saccharomyces cerevisiae*, one with a polyasparagine repeat (GFP^{N104}) and one without (GFP^{C}). Although both proteins can form microscopically visible GFP-positive aggregates, only the GFP^{N104}-containing aggregates exhibit morphological and biochemical characteristics that resemble the aggregates formed by mutant huntingtin in yeast cells. Formation of both the GFP^{C} and GFP^{N104} aggregates depends on microtubules, while only the GFP^{N104} aggregate requires the chaperone Hsp104 and the prion Rnq1 and is resistant to SDS. Although no microscopically visible GFP^{N104} aggregates were observed in the *hsp104*Δ and *rnq1*Δ mutant cells, SDS-insoluble aggregates can still be detected by the filter trap assay. These observations argue that the GFP^{N104}-containing aggregates can exist in at least two distinct states in vivo. We also show that a nucleus-targeted GFP^{N104} interferes with transcription from two SAGA-dependant promoters and results in a decrease in cell viability. Overall, the results imply that the GFP^{N104} protein behaves similarly to the mutant huntingtin in yeast cells and provides a new model for investigating the interplay between protein aggregates and the associated phenotypes.

INTRODUCTION

Protein aggregation is a distinct hallmark of many neurodegenerative diseases. Alzheimer's disease is associated with extracellullar amyloid plaques containing the Aβ peptide and intracellular neurofibrillary tangles of the tau protein.[1] In Parkinson's disease, degeneration of the dopaminergic neurons is accompanied by the formation of 'Lewy bodies', an intracellular protein inclusion that is composed primarily of α-synuclein.[2,3] The prion diseases in mammals are characterized by the presence of protease-resistant inclusions of the aggregated prion protein (PrP) in the central nervous system.[4] Protein aggregation is also a common characteristic of polyglutamine diseases, a family of neurodegenerative disorders caused by the expansion of a native glutamine tract within the affected proteins to a pathological length.[5,6] Because of the correlation between protein aggregation and cellular dysfunction and cell death in the neurodegenerative disorders, protein aggregates were initially thought to be the cause of the neuronal toxicity. However, recently studies have suggested that protein aggregation is not necessarily a requisite for cellular toxicity.[7,8] Furthermore, there is mounting evidence that formation of protein aggregates may shield the cell from more toxic, soluble form(s) of the affected protein.[9,10] Thus, the roles of protein aggregation in the initiation and progression of the cellular dysfunction in each neurodegenerative disorder needs to be re-examined and clarified.

A number of polypeptides comprising repetitive tracts of a single amino acid have been shown to be able to form aggregates both in vitro and in vivo. In solution, homopolymeric peptides of lysine, glutamate, and threonine can aggregate into amyloid fibrils that are microscopically similar to those formed by polyglutamine proteins.[11] When expressed in COS-7 cells, 11 of the 20 amino acids in a YFP-tagged homopolymer (X_{30}-YFP) formed aggregates.[12] Although there are many repetitive amino-acid sequences in the

human proteome, only polyalanine- and polyglutamine-containing proteins have been associated with diseases to date. In both cases, the disease state is caused by an expansion of the repetitive amino acid tract beyond the normal threshold in the native protein. The proteins affected in most of the known polyalanine diseases are transcription factors, and the disease phenotypes are thought to be caused by loss of function of the native proteins due to misfolding and aggregation of the expanded versions.[13] In contrast, the proteins affected in polyglutamine diseases share no similarity in cellular function, the types of neurons affected, or primary sequence except for the glutamine tract. Hence, the progressive neurodegenerative phenotypes shared by the polyglutamine diseases are believed to be caused by interference of normal cellular function by certain "gained" properties of the expanded glutamine tract rather than the loss of function of the native protein.[14] Consistent with this notion, insertion of a pathogenic length glutamine tract in the hypoxanthine phosphoribosyltransferase (Hprt) protein in a knock-in mouse model results in protein aggregation, behavioral abnormalities, and shortened life spans similar to the phenotypes observed in the mouse model of Huntington's Disease.[15,16] Polyglutamine proteins have been shown to exist in different oligomeric states both in vitro and in vivo,[17-19] and the roles of these different species of aggregates in pathogenesis are being actively investigated.

The budding yeast *Saccharomyces cerevisiae* has been successfully exploited as a model system for investigating protein aggregation and the associated cellular toxicity of a number of diseases. Characterization of the human α-synuclein in yeast has lead to the identification of a pathway that is potentially responsible for the cellular toxicity in Parkinson's disease.[20-22] Studies of the yeast prion Sup35 provided evidence for the first time that the prion form(s) of the protein may play a physiological role in cell function (e.g., adaptation to the changing environment).[23] Subsequently, the prion form of the human PrP protein has been implicated in the normal process of long-term memory formation.[24,25] Expression of a GFP-tagged, expanded N-terminal region (residues 1–68) of the human huntingtin (htt-NTD) in yeast cells produces protein aggregates that are insoluble in high concentrations of SDS, a shared characteristic of the polyglutamine aggregates in mammalian models.[26] In both yeast and mammalian cells, formation of the htt-NTD aggregate requires a functional microtubule system.[27] Moreover, protein chaperones such as the Hsp70 family members and the yeast Hsp104 are implicated in the formation and turnover of the protein aggregates in both yeast and mammalian cells.[26-30] One intriguing question is whether subcellular localization of the htt-NTD contributes to the observed cellular toxicity. It has been suggested that nuclear localization of the mutant htt-NTD in mammalian cells is required for its toxicity.[10,31] In yeast cells, nucleus targeting of the mutant htt-NTD results in altered transcription of a subset of genes and decreased cell viability.[32] When not specifically targeted to the nucleus, certain htt-NTD forms can still be toxic, although the toxicity of these htt-NTDs seems to be modulated by the sequences flanking the polyglutamine tract.[33] Thus, the role of subcellular localization of the mutant htt-NTD protein in cellular toxicity is not known.

Both glutamine and asparagine residues have side chains with terminal amides that can potentially form hydrogen bonds between repetitive residues. Hence, we surmise that polyasparagine and polyglutamine tracts may have a similar propensity to form aggregates. Interestingly, most of the characterized yeast prions contain a glutamine/asparagine-rich domain, which has been shown to be necessary and sufficient for prion formation.[34-37] In particular, the prion-forming domain of the yeast Ure2 is highly enriched in asparagine residues (26 of 64 amino acids) and deletion of this region greatly diminishes prion formation in vivo.[38] Here we report two constructs, one encoding a non-repetitive GFP-control protein (GFP^{C}) and the other a GFP-polyasparagine protein containing a N104 tract (GFP^{N104}), both of which give rise to microscopically visible aggregates when expressed in yeast cells. We demonstrate that the aggregates formed by GFP^{C} and GFP^{N104} are morphologically and physically distinct and have different effects on the cell. Although both aggregates are dependent on microtubule function, only the GFP^{N104} aggregates require the chaperone Hsp104 and the prion Rnq1 and are insoluble in a high concentration of SDS. In cells lacking Hsp104 or Rnq1, GFP^{N104} fails to form microscopically visible aggregates. However, the *hsp104*Δ and *rnq1*Δ mutant cells still have comparable levels of SDS-insoluble GFP^{N104} aggregates relative to the wild-type cells. Furthermore, we show that an NLS-tagged GFP^{N104} leads to a similar decrease in cell viability in both the wild-type and the *hsp104*Δ and *rnq1*Δ mutant strains, suggesting that the microscopically visible aggregates are not required for the observed toxicity. Finally, we demonstrate that the NLS-tagged GFP^{N104} can interfere with transcription from two promoters that are dependent on the SAGA (Spt-Ada-Gcn5-acetyltransferase) complex.[39] Our results clearly demonstrate that polyasparagine behaves similarly to polyglutamine in vivo. We propose that the oligomeric state of the protein and its subcellular localization play an important role in cellular toxicity. Given that the prion domain of yeast prions are asparagine rich and the prevalence of glutamine/asparagine rich proteins in the eukaryotic proteome,[40] understanding the contribution of polyasparagine tracts to protein aggregation and cell toxicity may provide important insight to protein aggregation related diseases.

MATERIALS AND METHODS

Strains and media. The *S. cerevisiae* strains used in this study were derived from BY4741 (*MATa his3*Δ *leu2*Δ *met15*Δ *ura3*Δ)[41] unless otherwise noted. ESM208 (*MAT*α *ura3-52 lys2-801 ade2-101 trp1*Δ*63 his3*Δ*200 leu2*Δ*1 tub4-1*) was a kind gift from Dr. Elmar Schiebel.[42] Genomic DNA from the W303 strain (*MATa can1-100 ade2-1 his3-11, 15 leu2-3, 112 trp1-1 ura3-1*) was used as a template for PCR amplification of the *HSP104* and *PHO84* promoters. For induction of the *GAL1* promoter, single colonies were grown overnight at 30°C in appropriate raffinose-containing selective complete media[43] to log-phase before addition of galactose to a final concentration of 2%. Benomyl (Sigma Aldrich) was used at a concentration of 20 μg/ml in dimethyl sulfoxide (DMSO).

Plasmids. Plasmid pMH858 is based on pRS314[44] and contains a DNA sequence encoding three copies of the Myc epitope (EQKLISEEDL) that is fused between the *RNR2* promoter and the entire *RNR2* coding sequence. The DNA sequence encoding the N-terminal region of Rnr2 (residues 1–297) in pMH858 was replaced with the sequence coding for a modified green fluorescent protein (GFP) optimized for yeast codon usage bias.[45] The nuclear localization signal (NLS) of the SV40 large T antigen[46] and the nuclear export signal (NES) of the mammalian MAPKK[46] were inserted between the Myc epitope sequence and the GFP coding sequence. The resulting

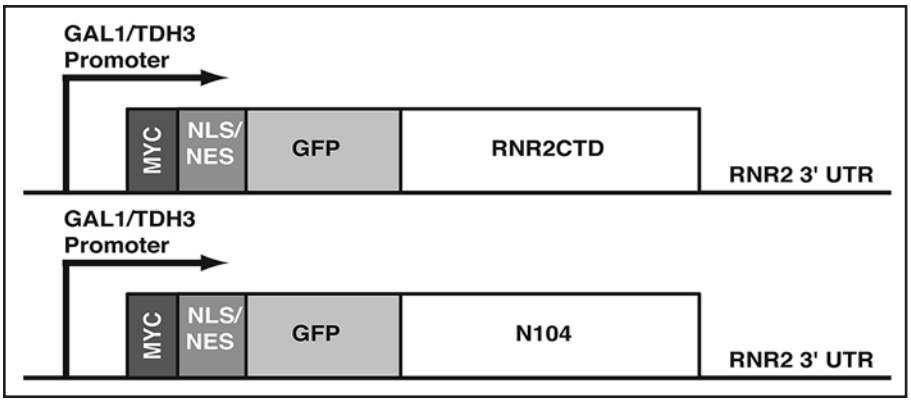

Figure 1. Schematic drawing of the GFP^C and GFP^{N104} constructs. The GFP^C construct encodes a GFP-RNR2CTD (amino acids 298–399) fusion protein with an N-terminal $(Myc)_3$ tag followed by the NLS or NES sequence. The GFP^{N104} construct contains a N104 tract in place of the RNR2CTD. All constructs encode proteins of similar sizes. The expression cassettes are put under the control of the galactose-inducible *GAL1* promoter or the constitutive *TDH3* promoter. All expression cassettes are flanked at the 3′ end by the *RNR2*'s 3′ UTR sequence.

constructs encode ~60 kD-size Myc_3-NLS-GFP-Rnr2CTD (residues 298–399) and Myc_3-NES-GFP-Rnr2CTD(residues 298–399), which are referred to as NLS-GFP^C and NES-GFP^C, respectively. The Rnr2CTD-endocing sequences in both the GFP^C constructs were replaced by an $(AATAAC)_{52}$ tract encoding 104 asparagine residues, yielding constructs expressing Myc_3-NLS-GFP-N104 (NLS-GFP^{N104}) and Myc_3-NES-GFP-N104 (NES-GFP^{N104}), both of similar sizes to the respective GFP^C proteins. All GFP^C and GFP^{N104} constructs were placed under the control of the inducible *GAL1* promoter and the constitutive *TDH3* promoter. The *HSP104-lacZ* (pMH960) and *PHO84-lacZ* (pMH963) reporter constructs each contained approximately 1 kb of the 5' untranslated regions of the respective genes fused upstream of the *LacZ* gene coding sequence in pRS416.[44]

Microscopy. GFP fluorescence was visualized in live cells by using a Nikon E-800 microscope (100X objective). Each experiment was performed in triplicate and ~150 cells were counted for each sample for statistical analyses. DNA was visualized by DAPI (4'6 diamidino-2-phenylindol·2HCl, Sigma) staining. Images were acquired with a Cool-SNAP-HQ 12-bit monochrome digital camera (Roper Scientific) by using the METAMORPH imaging software (Universal Imaging).

Protein extraction, filter trap assay and Western blotting. Protein extraction and the filter trap assay[47] were performed as described in Muchowski et al.[27] with minor modification. For most protein extract preparation, $1x10^8$ cells were resuspended in 150 µl of buffer H (50 mM HEPES pH7.5, 100 mM NaCl, 2.5 mM $MgCl_2$, 1 mM EGTA, and 5% Glycerol) supplemented with protease inhibitors (10 µg/ml antipain, 600 µg/ml aprotinin, 10 mM benzamidine, 10 µg/ml leupeptin, 10 µg/ml pepstatin A, 10 µg/ml soybean trypsin inhibitor, 100 mM PMSF, and 10 mM DTT). Cells were lysed by glass bead disruption on a Bead-beater (BioSpec). The lysates were transferred to a new tube and diluted with buffer H + 2% SDS. Samples were boiled for 10 min at 100°C and centrifuged at 16,100x g for 2 min, and the supernatant was collected for further analyses. For some of the filter trap assays, whole cell extracts (prepared by the same protocol but omitting the centrifugation step) were used in place of the supernatant fraction. Filter trap assays were performed by using a slot-blot or dot blot apparatus (BioRad) as described,[27] both 0.2 µm cellulose acetate (Schleicher & Schuell) and nitrocellulose membranes were equilibrated in buffer H + 0.1% SDS and washed twice with buffer H + 0.1% SDS before and after sample application. The membranes were blocked in TBST buffer (0.2 M TRIS base, 1.4 M NaCl, 0.1% Tween-20, pH-7.6) + 5% nonfat dry milk at 4°C overnight, incubated with the primary Ab 9E10 (1:1000, Covance) for 1 hour, and developed with peroxidase-labeled goat-anti-mouse Abs (1:10,000, Jackson Laboratory) by using an enhanced chemiluminescence substrate (PerkinElmer).

β-galactosidase assay. Cells were grown to log phase in liquid media before being harvested. Liquid β-galactosidase assays were performed on chloroform and SDS-permeabilized cells by using the colorimetric substrate *o*-nitrophenyhl-β-D-galactopyranoside (ONPG, Sigma) as previously described.[48] The β-galactosidase activities were measured in Miller units by using the following formula: $(1700*OD_{420}) /(\Delta T*OD_{600})$. All experiments were done in triplicate, and the average of each experiment was normalized against that of the appropriate vector control.

Plating viability assay. Cells were grown in selective glucose-containing media to log phase, harvested, and diluted to a final concentration of 5 cells/µl in water. The cell suspension was sonicated for 8 seconds by using a Branson Sonifier 250 at 20% output. Each strain was assayed in triplicate. For each sample, ~500 cells (100 µl) were separately plated on 2% glucose- and 2% galactose-containing solid selective media. Colonies were counted after two days (glucose) or four days (galactose) of incubation at 30°C.

Statistical analysis. The *p* values for the comparisons of interest were determined by a permutation (exact) test[49] by using the SAS statistical software version 9.1.3 (SAS Institute Inc; Cary, NC).

RESULTS

Both GFP^C and GFP^{N104} form visible aggregates. We controlled the expression of NLS- and NES-targeted, N-terminally Myc-tagged GFP^C and GFP^{N104} proteins (Fig. 1) in wild-type yeast cells by using the galactose-inducible *GAL1* promoter. Expression of the GFP^C and GFP^{N104} proteins were monitored via GFP fluorescence microscopy and cells were categorized into four groups based on their fluorescence pattern: (i) cells without any GFP signal; (ii) cells containing diffuse GFP signal (no foci); iii) cells containing one or more small (<1.5 µm) GFP foci (intermediate aggregates); (iv) cells containing 1–2 large (>1.5 µm) GFP foci (mature aggregates).

We originally designed the GFP^C expression constructs as control for non-aggregating proteins. Unexpectedly, both the GFP^C and GFP^{N104} proteins formed aggregates upon induced expression in yeast cells. After one hour of induction, aggregates (both intermediate and mature) were visible in over 60% of the cells expressing NLS-targeted GFP^C and GFP^{N104} (Fig. 2A). No statistically significant differences were observed in the percentage of aggregate-positive cells harboring the two proteins, and both remained above 60% throughout the 6-hour time course. Similarly, NES-targeted GFP^C and GFP^{N104} formed aggregates in >57% of the cells expressing the two proteins

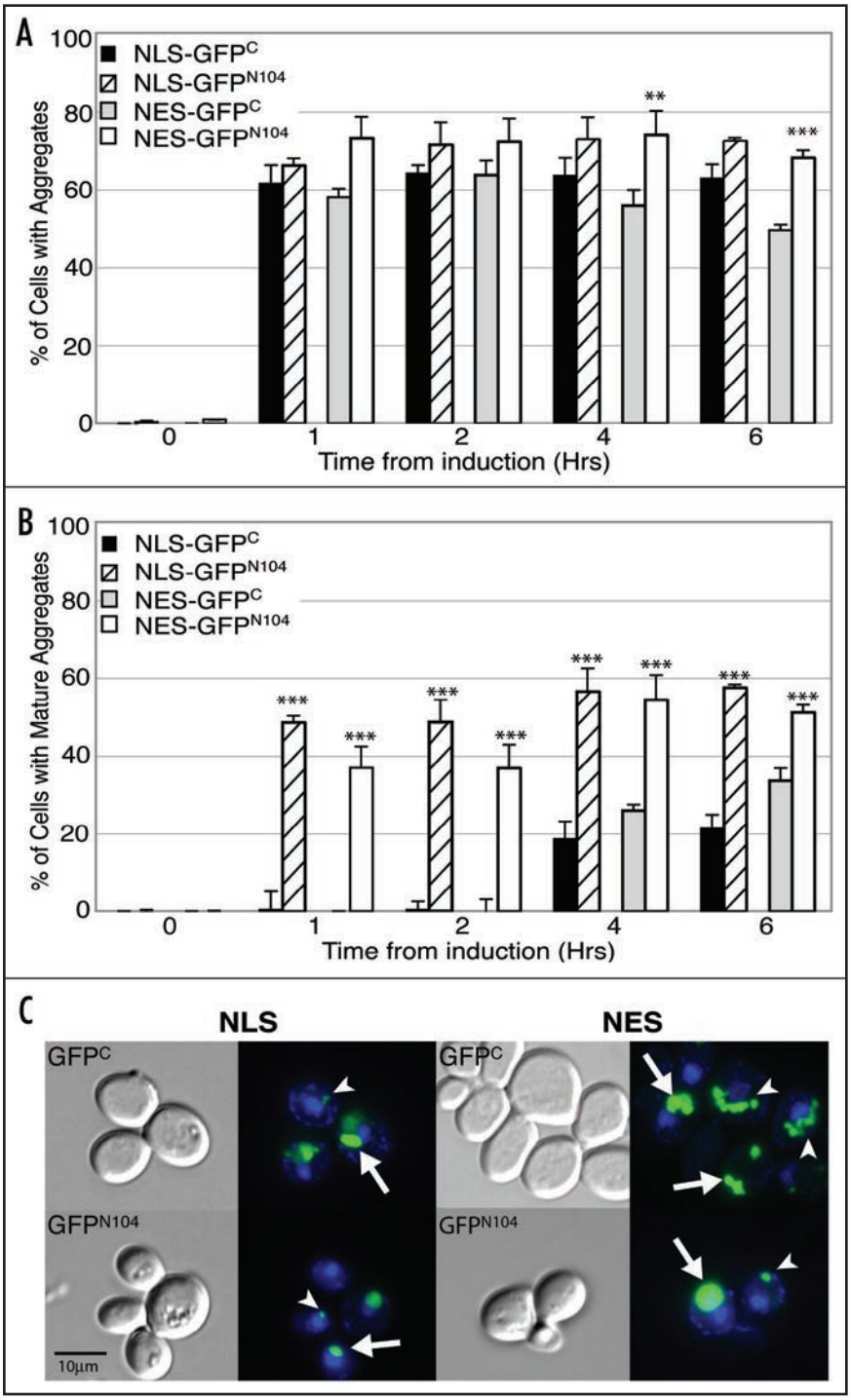

Figure 2. The GFP^{C} and GFP^{N104} proteins form morphologically distinct aggregates. Cells were grown to log phase in raffinose-containing media, and the expression of GFP^{C} or GFP^{N104} proteins were induced by addition of galactose. Cells were harvested right before the galactose addition (0 hrs), and at the indicated time points after induction. GFP signals were visualized microscopically in live cells, which were grouped into four categories based on their GFP patterns: (i) no GFP signal, (ii) diffuse GFP signal, (iii) intermediate aggregates (arrowhead), and (iv) mature aggregates (arrow). For each sample at least 150 cells were examined. (A) Percentage of cells that have either intermediate or mature aggregates. (B) Percentage of cells that have mature aggregates. (C) Images of GFP and DAPI signals in formaldehyde-fixed cells that were harvested four hours after induction. **p value ≤ 0.005, ***p value ≤ 0.001

within one hour of induction (Fig. 2A). Unlike the NLS-GFP^{C}, the percentage of cells with NES-GFP^{C} aggregates started to decrease after the 2-hour time point. In contrast, the percentage of cells with NES-GFP^{N104} aggregates remained above 68% throughout the 6-hour time course (Fig. 2A). Notwithstanding the differences, the level of aggregate-positive cells remained near or above 50% throughout the time course for all proteins tested, suggesting that a similar process may underlie the appearance of the microscopically visible aggregates regardless of the primary sequence of the proteins.

To determine the subcellular localization of the aggregates, we compared location of the GFP fluorescence to that of nuclear DNA stained by DAPI. Within 1-hour of induced expression, diffuse NLS-GFP^{C} and NLS-GFP^{N104} were visible in areas overlapping with the nuclear DAPI signal. Conversely, the NES-GFP^{C} and NES-GFP^{N104} proteins were dispersed throughout the cytoplasm (data not shown). At later time points, intermediate aggregates of NES-GFP^{C} and NES-GFP^{N104} appeared throughout the cytoplasm, while those of NLS-GFP^{C} and NLS-GFP^{N104} were restricted near the nucleus (Fig. 2C). Interestingly, the mature aggregates of both the NLS- and NES-targeted proteins were found predominately in the perinuclear region.

Aggregates of GFP^{C} and GFP^{N104} are morphologically different. Though both GFP^{C} and GFP^{N104} gave rise to comparable levels of aggregates in vivo, there were distinct differences in the types of aggregates each formed. The GFP^{C} protein formed primarily intermediate aggregates; cells with mature GFP^{C} aggregates were rarely detected until the 4-hour time point and remained below 35% of the population throughout the course of induction (Fig. 2B). Contrary to this observation, the GFP^{N104} proteins formed predominately mature aggregates throughout the time course. Within on hour of induction, mature aggregates were seen in 49% of the NLS-GFP^{N104} expressing cells and 37% of the NES-GFP^{N104} expressing cells (Fig. 2B). The percentage of cells with mature aggregates increased at later time points for both NLS-GFP^{N104} and NES-GFP^{N104}, resulting in significant differences from the respective GFP^{C} proteins (Fig. 2B).

The mature aggregates formed by GFP^{C} and GFP^{N104} also differ morphologically. For both NLS and NES-targeted proteins, the mature aggregates of GFP^{N104} were tight spherical foci, whereas those of GFP^{C} were more irregular in shape and resembled a large conglomeration of smaller aggregates (Fig. 2C). The distinction in morphology may suggest differences in physical properties of the GFP^{C} and GFP^{N104} aggregates. Notably, the compact foci in cells expressing GFP^{N104} are reminiscent of the aggregates formed by the mutant htt-NTD in yeast cells,[26,32,50] indicating similar mechanisms for the aggregation of polyasparagine and polyglutamine proteins.

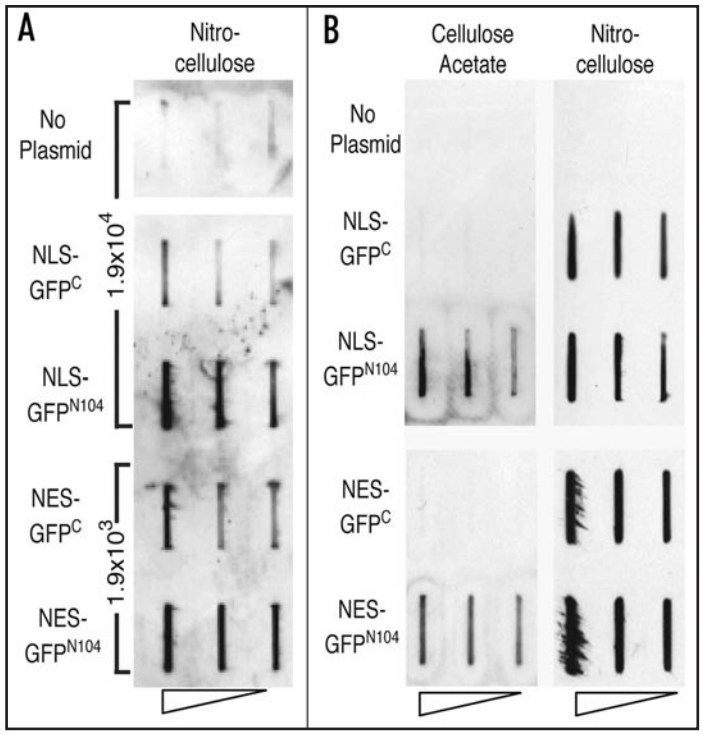

Figure 3. Detection of SDS-insoluble aggregates in the supernatant fraction of lysates of the GFP^{N104}-expressing cells by the filter trap assay. Cells were grown to log phase in raffinose-containing media, induced for GFP^{C} and GFP^{N104} expression by addition of galactose, and harvested for lysis after 5 hours. (A) Cell lysates were supplemented with SDS to a final concentration of 2% and boiled for 10 min at 100°C. Cell lysates were diluted with buffer H supplemented with 2% SDS according to the number of cells of each sample before being loaded onto a nitrocellulose membrane and subjected to Western blotting by using the monoclonal anti-Myc antibody 9E10. The number of cells loaded in the first well is indicated, with two-fold dilution in the subsequent wells. (B) Supernatant fractions were prepared from cell lysates by centrifugation at 16,100 xg for 2 min. Supernatant fractions were diluted and loaded onto cellulose acetate (left panel) and nitrocellulose (right panel) membranes empirically so as to yield comparable signal on the nitrocellulose membrane between the GFP^{C} and GFP^{N104} samples, with two-fold dilution in subsequent wells.

The GFP^{N104} aggregates are SDS-insoluble. An important characteristic of the protein aggregates found in Huntington's, Parkinson's, and Alzheimer's disease is their insolubility in high concentrations (≥2%) of SDS.[17,19,51] We found that the GFP^{N104} proteins were trapped at the interface of the stacking and separating gels in SDS/PAGE, even after the cell lysates were boiled in a buffer containing 2% SDS (data not shown), suggesting the presence of SDS-insoluble aggregates. To further determine if GFP^{N104} could form SDS-resistant aggregates, we used a cellulose acetate membrane based filter trap assay to detect SDS-insoluble protein oligomers that were larger than 0.2 μm in solution.[47,52,53] When the supernatant fractions of the whole cell lysates from equal number of cells were analyzed by this assay, a significant amount of the GFP^{N104}, but not the GFP^{C} proteins, was retained on the cellulose acetate membrane (data not shown). Interestingly, blotting of protein extracts of the supernatant fraction and the whole cell lysates onto a nitrocellulose membrane revealed that steady state levels of the GFP^{C} proteins were much lower than those of the GFP^{N104} proteins (Fig. 3A). Because both GFP^{C} and GFP^{N104} are under the control of the same promoter, the observed different protein levels may reflect a difference in stability of the two proteins. When the supernatant fraction was adjusted to allow loading of equal amount of the GFP^{C} and GFP^{N104} proteins, significant levels of the GFP^{N104} proteins were observed on the cellulose acetate membrane while virtually no GFP^{C} proteins were seen (Fig. 3B). Our results suggest that the GFP^{N104}, but not the GFP^{C} proteins, are capable of forming SDS-resistant protein aggregates inside the cell.

Formation of both the GFP^{C} and GFP^{N104} aggregates depends on microtubules. The protein aggregates seen in polyglutamine diseases have in some cases been classified as aggresomes, which are defined as perinuclear protein aggregates that are formed via microtubule-mediated retrograde transport and enveloped by the intermediate filament vimentin in mammalian cells.[54,55] Disruption of the microtubule cytoskeleton or microtubule-mediated transport can inhibit aggresome formation in mammalian cells.[56,57] It has been postulated that a similar structure can form when the mutant htt-NTD is expressed in yeast cells, as htt-containing aggregates form perinuclearly and require microtubules.[27] To examine the role of microtubules in aggregation of GFP^{C} and GFP^{N104}, we characterized the aggregation of the two proteins in wild-type cells treated with the microtubule-depolymerizing agent benomyl, as well as in the temperature-sensitive *tub4-1* mutant cells that have a defective γ-tubulin at restrictive temperatures. Treatment of benomyl effectively abolished both the NLS-GFP^{C} and the NES-GFP^{C} aggregates, and greatly diminished the levels of the NLS-GFP^{N104} (from 50% to 2.9%) and NES-GFP^{N104} (from 55% to 12%) aggregates (Fig. 4A). Similarly, shifting of the *tub4-1* cells from 22°C (permissive temperature) to 37°C (restrictive temperature) also led to significant decreases in the levels of NLS-GFP^{C} (from 16% to 3.1%) and NES-GFP^{C} (from 27% to 1.6%) aggregates, as well as those of the NLS-GFP^{N104} (from 30% to 8.8%) and NES-GFP^{N104} (from 51% to 0.6%) aggregates (Fig. 4B). Taken together, our results indicate that microtubules are important to the formation of the mature aggregates of both GFP^{C} and GFP^{N104}.

Hsp104 and Rnq1 are required for formation of the microscopically visible but not the SDS-insoluble GFP^{N104} aggregates. Protein chaperones have been shown to play a critical role in the pathogenesis of aggregation-associated disorders.[28,30,50,58] Overexpression of Hsp104 in yeast cells can shift a GFP-fused mutant htt-NTD from large-aggregate to small-aggregate or diffuse states.[26] Conversely, deletion of the *HSP104* gene abolishes foci formation of the GFP-tagged htt-NTD[26,59] in the cytoplasm. Therefore, it would appear that Hsp104 participates in both the aggregation and turnover of the aggregates of the mutant htt-NTD. Hsp104 likely mediates aggregation of the mutant htt-NTD through Rnq1, as Hsp104 is essential for maintaining the prion state of *[RNQ^{+}]*, which is subsequently required for aggregation of the mutant htt-NTD.[59] Interestingly, however, when htt-NTD is targeted to the nucleus in *hsp104*Δ cells, SDS-insoluble aggregates are still detectable.[60]

We examined the roles of Hsp104 and Rnq1 in GFP^{C} and GFP^{N104} aggregation by microscopically monitoring aggregate formation in wild-type and the *hsp104*Δ and *rnq1*Δ mutant cells. While no decrease in aggregation of the NLS-GFP^{C} and NES-GFP^{C} proteins was observed between the wild-type and the *hsp104*Δ or *rnq1*Δ mutant cells, there was a significant reduction in levels of mature aggregates of both the NLS- and NES-GFP^{N104} proteins in the two mutants. The level of mature NLS-GFP^{N104} aggregates was significantly reduced in the *hsp104*Δ mutant relative to the

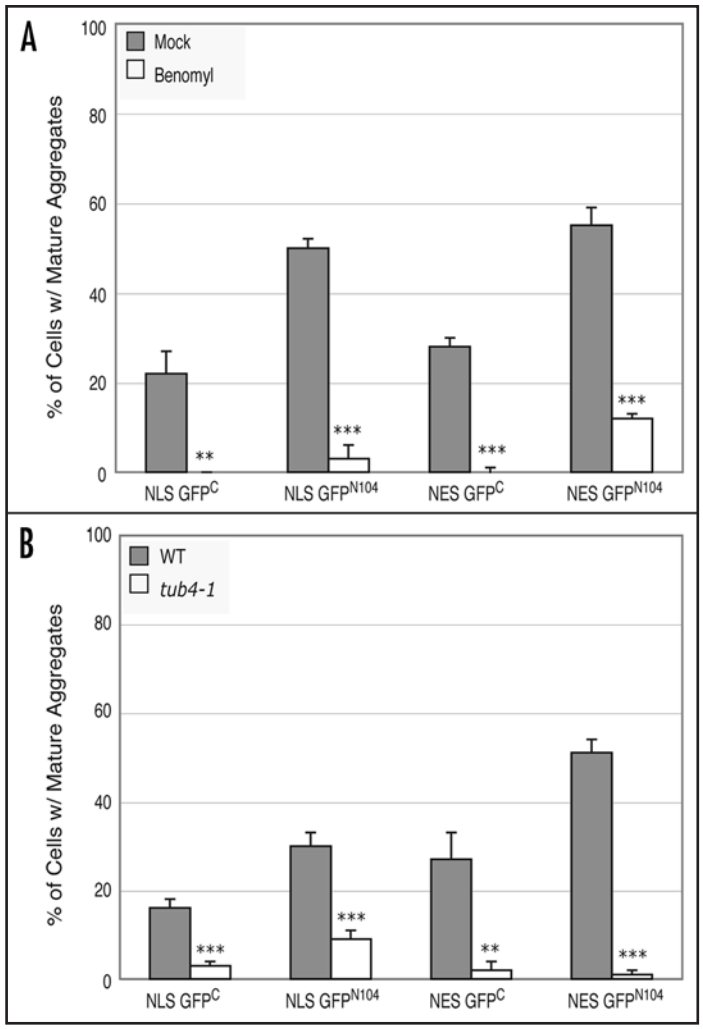

Figure 4. Formation of both the GFP^{C} and GFP^{N104} aggregates require microtubule function. (A) Disruption of aggregation by benomyl. Cells were grown to log phase in a raffinose-containing medium, split into two halves, and the expression of GFP^{C} or GFP^{N104} were induced by addition of galactose in the presence of benomyl in DMSO or DMSO alone. The percentage of cells containing mature aggregates was determined 6 hours after benomyl/DMSO treatment. (B) Disruption of aggregates by a defective γ-tubulin. Wild-type and *tub4-1* cells were grown in a raffinose-containing medium to log phase at 22˚C, and immediately shifted to 37˚C upon the induction of GFP^{C} and GFP^{N104} expression by addition of galactose. Cells were examined for the presence of mature aggregates 6 hours after the galactose induction and temperature shift. **p value ≤ 0.005, ***p value ≤ 0.001.

wild-type cells (1.9% versus 57%) (Fig. 5A). The level of the mature NES-GFP^{N104} aggregates was also lower in *hsp104*Δ relative to wild-type cells, although the difference is less dramatic (17% versus 58%). Similarly, *rnq1*Δ cells expressing the NLS-GFP^{N104} and NES-GFP^{N104} proteins also exhibited significantly lower levels of mature aggregates relative to the wild-type cells (20% versus 57% for NLS-GFP^{N104} and 6% versus 58% for NES-GFP^{N104}) (Fig. 5A). The decrease in the levels of the mature GFP^{N104} aggregates in the *hsp104*Δ and *rnq1*Δ mutant cells was unlikely due to decrease in protein levels since there was a higher percentage of GFP-positive cells in both the mutants than in the wild-type control (data not shown). Moreover, in both the mutants there was a proportional increase in the percentage of cells with diffuse GFP^{N104} signals accompanying the decrease in cells containing mature GFP^{N104} aggregates in comparison to the wild-type strain (Fig. 5B). Unlike the GFP^{N104} proteins, no significant increase was observed in the levels of diffuse GFP^{C} signals between the wild-type, *hsp104*Δ, and *rnq1*Δ cells (Fig. 5B).

We next asked whether the decrease in the GFP^{N104} aggregates in the *hsp104*Δ and *rnq1*Δ mutants was accompanied by a similar decrease in the level of SDS-insoluble aggregates as detected by the filter trap assay. Unexpectedly, both NLS-GFP^{N104} and NES-GFP^{N104} led to similar levels of SDS-insoluble aggregates in the *hsp104*Δ and *rnq1*Δ cells relative to the wild-type cells (Fig. 5C). These results suggest that there are at least two species of the GFP^{N104} aggregates in vivo; one is larger and visible under the light microscope and the other is smaller than the detection threshold of light microscopy but detectable by the filter trap assay. We conclude that the Hsp104 and Rnq1 proteins, while required for formation of the microscopically visible aggregate species, are not essential for the formation of the smaller SDS-insoluble species.

A nucleus-targeted GFP^{N104} leads to decreased cell viability. Previous studies suggest that the mutant htt-NTD can compromise cell viability when expressed in yeast cells depending on the amino acid sequences flanking the htt-NTD or the subcellular localization of the fusion protein.[32,33] In some cases, the cellular toxicity seems to depend on a FLAG epitope attached to the mutant htt-NTD.[33] On the other hand, when the mutant htt-NTD is targeted to the nucleus by fusion of the NLS of the SV40 large T antigen, it can cause a decrease in cell viability in the absence of the FLAG epitope.[32] We examined the effect of the GFP^{C} and GFP^{N104} proteins on cell viability by comparing plating efficiency of cells harboring *GAL1*-driven, NES- or NLS-tagged GFP^{C} and GFP^{N104} constructs, as well as cells harboring the blank vector control, between induced (galactose-containing media) and repressed (glucose-containing media) conditions. No significant difference was observed between NES-GFP^{C} and NLS-GFP^{C} relative to the vector control. Likewise, there was no significant difference between cells expressing NES-GFP^{N104} and the vector control (Fig. 6A). In contrast, cells expressing the NLS-GFP^{N104} protein exhibited a significantly lower viability relative to cells expressing the NLS-GFP^{C} (64 versus 94%) (Fig. 6A). Our results suggest that the NES-GFP^{C}, NES-GFP^{N104}, and the NLS-GFP^{C} proteins are not toxic to yeast cells despite the large microscopically visible aggregates that they form. Moreover, the difference in viability between cells expressing the NLS-GFP^{N104} and the NES-GFP^{N104} suggests that nuclear localization of the GFP^{N104} protein is required for the observed cellular toxicity.

Recently studies suggest a positive correlation between microscopically visible aggregates and cellular toxicity mediated by the mutant-htt NTD in yeast cells.[59,61] To determine if this is the case for the NLS-GFP^{N104} mediated toxicity, we compared viability of the wild-type and the *hsp104*Δ and *rnq1*Δ mutant cells expressing NLS-GFP^{N104}. Despite the decrease in levels of the microscopically visible NLS-GFP^{N104} aggregates in the *hsp104*Δ and *rnq1*Δ mutant cells (Fig. 5A), there was no significant difference in the levels of decrease in cell viability between the two mutants and the wild type (Fig. 6B). In addition, NES-GFP^{N104} had no significant effect on the viability of the *hsp104*Δ or *rnq1*Δ mutants, as was the case of the wild-type strain (data not shown). These observations suggest that that the decrease in the level of the microscopically visible NLS-GFP^{N104}

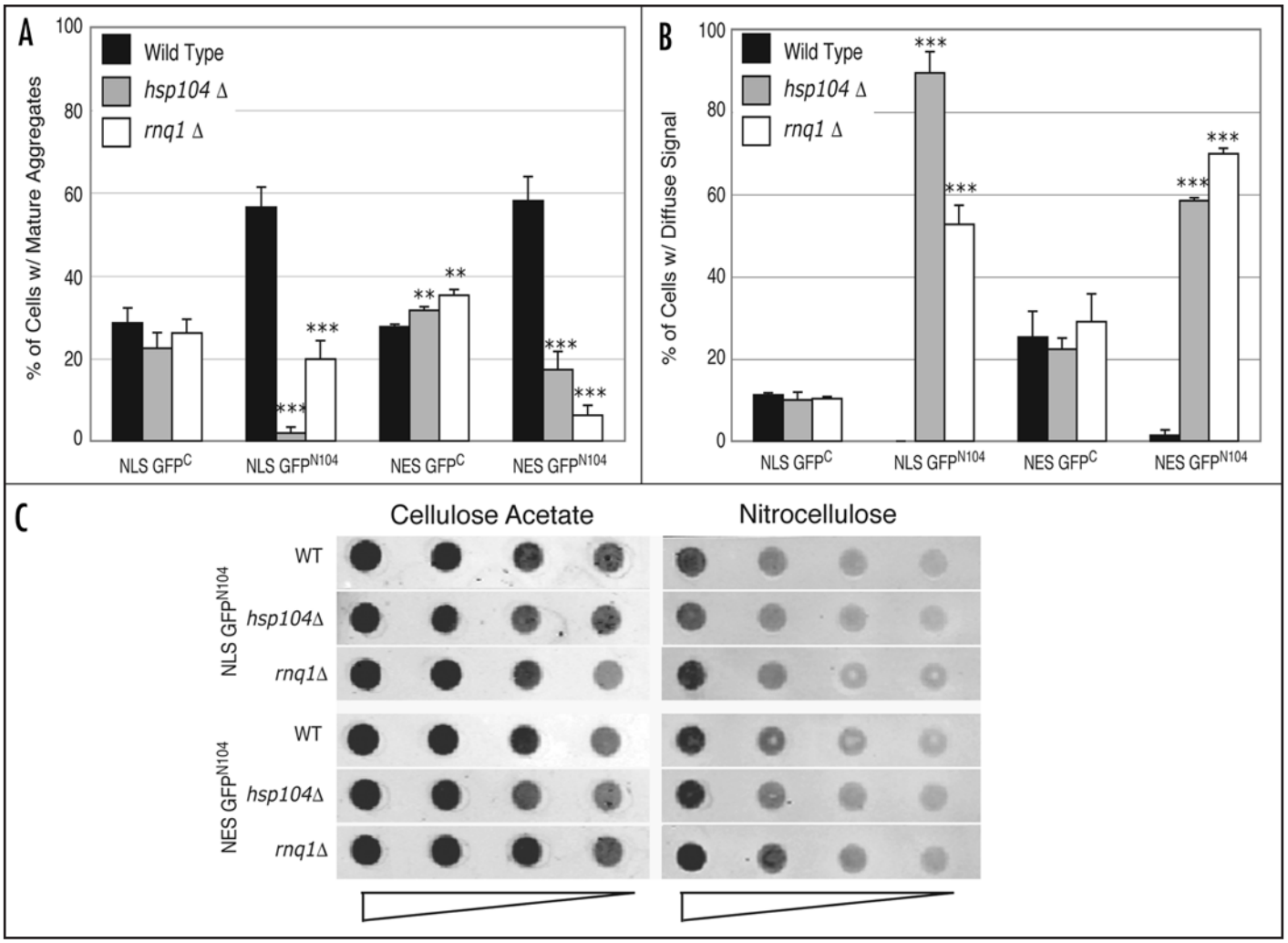

Figure 5. *HSP104* and *RNQ1* are required for formation of the microscopically visible aggregates. Wild-type, *hsp104Δ*, and *rnq1Δ* cells were grown in a raffinose-containing medium to log phase before addition of galactose to induce expression of the GPF^{C} and GFP^{N104} proteins. Cells were harvested at the 6-hour time point after induction and their GFP patterns were categorized as described in Figure 2 legend. (A) Percentage of cells containing mature aggregates. (B) Percentage of cells containing diffuse GFP signals. (C) Comparison of levels of SDS-insoluble aggregates between the wild-type and the *hsp104Δ* and *rnq1Δ* mutant cells by a dot blot filter trap assay. Induced expression of NLS-GFP^{N104} and NES-GFP^{N104} and supernatant preparation from total cell lysates were as described in Figure 3 legend. The number of cells loaded in the first well was empirically determined to result in similar Western blot signals between strains on the nitrocellulose membrane, and the extract was subjected to two-fold serial dilutions in the subsequent wells. **p value ≤ 0.005, ***p value ≤ 0.001.

aggregates does not correlate with increased cell viability.

NLS-GFP^{N104} compromises transcription from the *PHO84* and *HSP104* promoters. In some cellular models of polyglutamine diseases, proteins with a expanded polyglutamine tract have been shown to cause transcriptional dysregulation before onset of symptoms.[62] Alteration of transcriptional profiles has also been reported for yeast cells expressing the mutant htt-NTD.[32] While transcripts of genes encoding chaperones and heat-shock proteins were induced by presence of the mutant htt-NTD irrespective of its subcellular localization, significant transcriptional repression was observed only when the mutant protein is targeted to the nucleus.[32] We examined the possible effect of the NLS-GFP^{N104} protein on transcription from two promoters; one is the *PHO84* promoter that is repressed by the nucleus-targeted mutant htt-NTD, and the other is the *HSP104* promoter that is induced by both the nuclear and cytoplasmic expression of the mutant htt-NTD.[32] Incidentally, transcription from both the promoters is regulated by the SAGA complex, which is involved in modulating expression of ~10% of the genes in the yeast genome.[63,64] We found that constitutive expression of the NLS-GFP^{N104} protein resulted in decreased transcription from both the *PHO84* (5-fold) and the *HSP104* (2.4-fold) promoters (Fig. 7). On the other hand, expression of the NLS-GFP^{C} led to no significant change in transcription from the *PHO84* promoter and only a slight increase (1.7-fold) in transcription from the *HSP104* promoter (Fig. 7). No significant difference in transcription was observed from the *PHO84* or *HSP104* promoters in the presence of NES-GFP^{C} or NES-GFP^{N104} (data not shown).

DISCUSSION

This work describes the use of a yeast model system to investigate aggregating proteins and their effects upon the cell. We have examined two proteins, GFP^{C} and GFP^{N104}, both of which can form aggregates when targeted to the cytoplasm and the

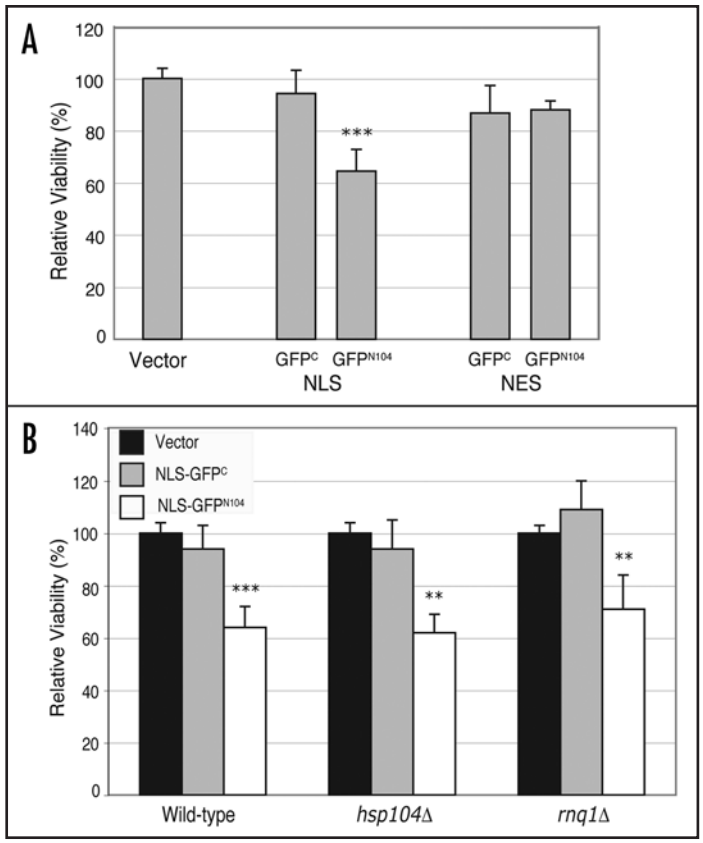

Figure 6. A nucleus-targeted GFP^{N104} results in decreased cell viability. Wild-type, *hsp104*Δ and *rnq1*Δ cells carrying the control vector or plasmids encoding galactose-inducible, NLS or NES-tagged GFP^{C} and GFP^{N104} were grown to mid-log phase under repressed conditions. Cultures were diluted and ~500 cells were plated on appropriate selective media containing either glucose (repressed) or galactose (induced) as the carbon source. The numbers of colonies were counted after 48-hour (glucose) or 96-hour (galactose) incubation at 30˚C. Viability of cells bearing each plasmid was calculated as the quotient of the number of colonies on the galactose plate divided by the number of colonies on the glucose plate. For each strain, the viabilities of cells expressing GFP^{C} and GFP^{N104} were normalized against the viability of cells harboring the vector alone, yielding the relative viability. (A) Comparison of viability between wild-type cells containing the vector control, the NLS-tagged GFP^{C} and GFP^{N104}, and the NES-tagged GFP^{C} and GFP^{N104}. (B) Comparison of the effect of NLS-GFP^{C} and NLS-GFP^{N104} on cell viability relative to the vector control in wild-type, *hsp104*Δ and *rnq1*Δ strains. **p value ≤ 0.005, ***p value ≤ 0.001.

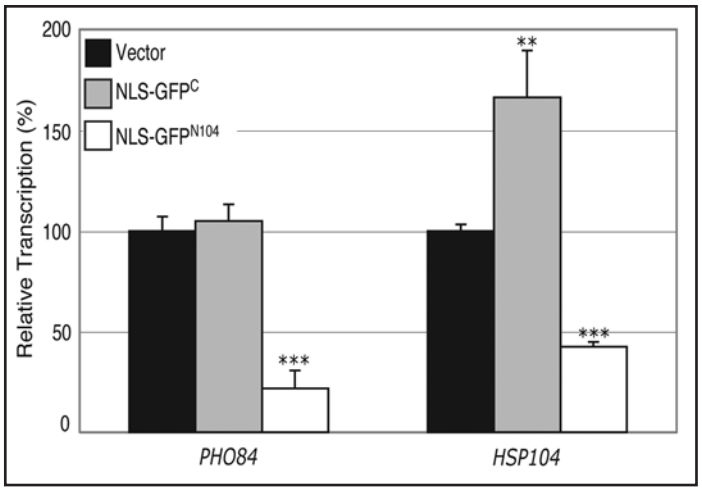

Figure 7. NLS-GFP^{N104} compromises transcription from the *PHO84* and *HSP104* promoters. Transcription from the *PHO84* and *HSP104* promoters was examined by measuring β-galactosidase activity resulting from the *PHO84-lacZ* and *HSP104-lacZ* reporter plasmids, respectively, in wild-type cells expressing NLS-GFP^{C} or NLS-GFP^{N104} from the constitutive *TDH3* promoter. The β-galactosidase values were normalized against those from cells carrying the control vector alone, yielding the relative transcription. **p value ≤ 0.005, ***p value ≤ 0.001.

nucleus of yeast cells. However, the aggregates formed by the two proteins are fundamentally different. Of the two, only the GFP^{N104} aggregates exhibit biochemical and phenotypic characteristics that are reminiscent of those attributed to expression of the mutant htt-NTD in yeast cells.[26,27] Similar to the mutant htt-NTD, the GFP^{N104} proteins forms large and compact aggregates (1~2 per cells) that can be observed under a light microscope within one hour of induced expression. Importantly, the formation of these GFP^{N104} aggregates requires the microtubules as well as the protein chaperone Hsp104 and the prion Rnq1, as is the case of the mutant htt-NTD. Moreover, both the GFP^{N104} proteins and the mutant htt-NTD can form SDS-insoluble aggregates that can be detected in the supernatant fraction of cell lysates. We have also shown that targeting GFP^{N104} to the nucleus results in decreased cell viability and compromises transcription, a phenomenon previously reported for a nucleus-targeted mutant htt-NTD.[32]

A polyasparagine peptide was shown to form β-pleated sheets in solution, similar to that of a polyglutamine peptide of similar length.[65] In the three known yeast prion proteins (Sup35, Rnq1 and Ure2), a glutamine/asparagine-rich domain is both necessary and sufficient for establishing and aggregating the prion form of each protein in vivo.[34-36] Our finding that the polyasparagine-containing GFP^{N104} protein recapitulates the morphological and biochemical characteristics of the mutant htt-NTD in vivo provides direct evidence that polyasparagine, like polyglutamine, can form aggregates and interfere with cellular function, possibly through a similar mechanism. Thus, it would appear that asparagine residues can play an important role in aggregation of the yeast prion proteins as well as other glutamine/asparagine-rich proteins.

We find that both the NES-GFP^{C} and NES-GFP^{N104} proteins tend to form aggregates at the peripheral regions of the nucleus and that both aggregations depend on microtubules. Perinuclear localization of aggregates and microtubule-dependent aggregation are hallmarks of aggresomes.[54,55] Formation of an aggresome is postulated to be an intermediate step in the turnover of misfolded or partially denatured proteins by the lysosome via autophagy.[57] Considerable evidence suggests that the mutant htt-NTD can form aggresomes both in mammalian cells[29,66] and in yeast,[27] and is degraded in the lysosome in mammalian cells.[56,66,67] Our results suggest that overload of yeast cells with the GFP^{C} or GFP^{N104} proteins may lead to formation of aggresome-like structures as a cellular response to dispose of the protein.

In this study we use two different methods to characterize the presence and level of protein aggregation: one by fluorescence microscopy in live cells to visualize GFP-positive aggregates, and the other by filter trap assay to detect protein aggregates that are insoluble in 2% of SDS in the supernatant fraction of whole-cell lysates. These two approaches likely detect two different forms

of aggregates in the cell. For example, the filter trap assay fails to detect any SDS-insoluble aggregates of the GFP^{C} proteins, although GFP-positive aggregates can be readily observed by microscopy. In the case of GFP^{N104}, while the levels of microscopically visible aggregates are greatly diminished in the *hsp104*Δ and *rnq1*Δ mutants as compared to the wild-type cells, the levels of SDS-insoluble aggregates remain similar between the mutants and the wild type. Thus the type of aggregates revealed by the filter trap assay in the *hsp104*Δ and *rnq1*Δ mutant cells cannot be detected at all by fluorescence microscopy. Our present in vivo studies may help elucidate how different states of protein aggregation may contribute to cellular toxicity in the neurodegenerative diseases.

We have shown that expression of the NLS-GFP^{N104} results in the same level of decrease in cell viability in the *hsp104*Δ, and *rnq1*Δ mutant cells as in the wild-type cells. Likewise, the level of SDS-insoluble aggregates is similar between the wild-type and mutant strains. It thus appears that the aggregates detected by the filter trap assay, rather than the microscopically visible aggregates, may play a major role in cellular toxicity seen here. This is in contrast to a previous study showing a correlation between decreased levels of microscopic aggregates and reduced toxicity of a "toxic" htt-NTD construct expressed in yeast cells.[33,59] Interestingly, the toxic htt-NTD protein forms smaller amorphous aggregates that are morphologically distinct from the GFP^{N104} aggregates seen in this study.[33] Notably, only the non-toxic mutant htt-NTD constructs are shown to form tight spherical aggregates similar to the GFP^{N104} aggregate shown here.[26,33,53] The pathways leading to these different forms of aggregates and their roles in mediating cellular toxicity is an area of active investigation.

The molecular analysis of the GFP^{N104} aggregates described here raises some intriguing questions on the role of Hsp104 and Rnq1 in aggregate formation. The Hsp104 and Rnq1 proteins are both required to maintain the [RNQ^{+}] prion state,[59,68] which was previously shown to be essential to "seed" microscopically-visible aggregates of both the Sup35 prion[69] and mutant huntingtin[33,61] in yeast cells. The wild-type strain used in this study is S288C, which has been shown to be [RNQ^{+}].[33,59] We have shown that formation of the microscopically visible GFP^{N104} aggregates depends on both Rnq1 and Hsp104, suggesting that these aggregates also require a [$RNQ1^{+}$] prion state. On the other hand, formation of the SDS-insoluble class of aggregates seems to occur independent of *HSP104* and *RNQ1.* Thus it would appear that aggregation of the GFP^{N104} protein occurs in at least two steps. The initial step involves formation of SDS-resistant smaller oligomers. This step, apparently *HSP104* and *RNQ1* independent, could be mediated by self-association between the polyasparagine residues given the propensity of asparagine polypeptides to aggregate in vitro.[11,12,65] We propose that the later step(s) of aggregation involve formation of the larger aggregates, which requires both functioning microtubules and the Hsp104 and Rnq1 proteins.

We show that the GFP^{N104}-mediated decrease in cell viability requires its nuclear localization. A similar correlation between nuclear localization and toxicity was previously reported for a polyglutamine protein in mammalian cells.[10,70] The mutant huntingtin was shown to interact with a number of transcription factors that contain glutamine- or asparagine-rich regions.[52,71-75] This interaction is believed to compromise the normal function of these transcription factors, which may in part contribute to the cellular toxicity.[53,72-74] In yeast cells, a nucleus-targeted mutant htt-NTD was also shown to alter transcription from many promoters, particularly those regulated by the SAGA complex.[32] Evidently, several components of the yeast SAGA complex contain domains that are enriched in glutamine/asparagine residues.[76,77] Here we show that the NLS-GFP^{N104} protein can affect transcription from two SAGA-regulated promoters. It is possible that NLS-GFP^{N104} may associate with some of the glutamine/asparagine-rich SAGA components, thereby compromising their normal activity. Further studies are required to determine whether compromised transcription of the SAGA-regulated genes contributes to the decrease in cell viability.

References

1. Selkoe DJ. Cell biology of protein misfolding: The examples of Alzheimer's and Parkinson's diseases. Nat Cell Biol 2004; 6:1054-61.
2. Cookson MR. Pathways to Parkinsonism. Neuron 2003; 37:7-10.
3. McNaught KS, Shashidharan P, Perl DP, Jenner P, Olanow CW. Aggresome-related biogenesis of Lewy bodies. Eur J Neurosci 2002; 16:2136-48.
4. Fornai F, Ferrucci M, Gesi M, Bandettini di Poggio A, Giorgi FS, Biagioni F, Paparelli A. A hypothesis on prion disorders: Are infectious, inherited, and sporadic causes so distinct? Brain Res Bull 2006; 69:95-100.
5. Zoghbi HY, Orr HT. Glutamine repeats and neurodegeneration. Annu Rev Neurosci 2000; 23:217-47.
6. Nakamura K, Jeong SY, Uchihara T, Anno M, Nagashima K, Nagashima T, Ikeda S, Tsuji S, Kanazawa I. SCA17, a novel autosomal dominant cerebellar ataxia caused by an expanded polyglutamine in TATA-binding protein. Hum Mol Genet 2001; 10:1441-8.
7. Chui DH, Tanahashi H, Ozawa K, Ikeda S, Checler F, Ueda O, Suzuki H, Araki W, Inoue H, Shirotani K, Takahashi K, Gallyas F, Tabira T. Transgenic mice with Alzheimer presenilin 1 mutations show accelerated neurodegeneration without amyloid plaque formation. Nat Med 1999; 5:560-4.
8. Tagawa K, Hoshino M, Okuda T, Ueda H, Hayashi H, Engemann S, Okado H, Ichikawa M, Wanker EE, Okazawa H. Distinct aggregation and cell death patterns among different types of primary neurons induced by mutant huntingtin protein. J Neurochem 2004; 89:974-87.
9. Arrasate M, Mitra S, Schweitzer ES, Segal MR, Finkbeiner S. Inclusion body formation reduces levels of mutant huntingtin and the risk of neuronal death. Nature 2004; 431:805-10.
10. Saudou F, Finkbeiner S, Devys D, Greenberg ME. Huntingtin acts in the nucleus to induce apoptosis but death does not correlate with the formation of intranuclear inclusions. Cell 1998; 95:55-66.
11. Fandrich M, Dobson CM. The behaviour of polyamino acids reveals an inverse side chain effect in amyloid structure formation. Embo J 2002; 21:5682-90.
12. Oma Y, Kino Y, Sasagawa N, Ishiura S. Intracellular localization of homopolymeric amino acid-containing proteins expressed in mammalian cells. J Biol Chem 2004; 279:21217-22.
13. Albrecht A, Mundlos S. The other trinucleotide repeat: Polyalanine expansion disorders. Curr Opin Genet Dev 2005; 15:285-93.
14. Orr HT. Beyond the Qs in the polyglutamine diseases. Genes Dev 2001; 15:925-32.
15. Ordway JM, Tallaksen-Greene S, Gutekunst CA, Bernstein EM, Cearley JA, Wiener HW, Dure LST, Lindsey R, Hersch SM, Jope RS, Albin RL, Detloff PJ. Ectopically expressed CAG repeats cause intranuclear inclusions and a progressive late onset neurological phenotype in the mouse. Cell 1997; 91:753-63.
16. Tallaksen-Greene SJ, Ordway JM, Crouse AB, Jackson WS, Detloff PJ, Albin RL. *Hprt(CAG)146* mice: Age of onset of behavioral abnormalities, time course of neuronal intranuclear inclusion accumulation, neurotransmitter marker alterations, mitochondrial function markers, and susceptibility to 1-methyl-4-phenyl-1,2,3,6-tetrahydropyridine. J Comp Neurol 2003; 465:205-19.
17. Ellisdon AM, Thomas B, Bottomley SP. The two-stage pathway of ataxin-3 fibrillogenesis involves a polyglutamine-independent step. J Biol Chem 2006; 281:16888-96.
18. Hoffner G, Island ML, Djian P. Purification of neuronal inclusions of patients with Huntington's disease reveals a broad range of N-terminal fragments of expanded huntingtin and insoluble polymers. J Neurochem 2005; 95:125-36.
19. Iuchi S, Hoffner G, Verbeke P, Djian P, Green H. Oligomeric and polymeric aggregates formed by proteins containing expanded polyglutamine. Proc Natl Acad Sci USA 2003; 100:2409-14.
20. Griffioen G, Duhamel H, Van Damme N, Pellens K, Zabrocki P, Pannecouque C, van Leuven F, Winderickx J, Wera S. A yeast-based model of α-synucleinopathy identifies compounds with therapeutic potential. Biochim Biophys Acta 2006; 1762:312-8.
21. Dixon C, Mathias N, Zweig RM, Davis DA, Gross DS. Alpha-synuclein targets the plasma membrane via the secretory pathway and induces toxicity in yeast. Genetics 2005; 170:47-59.
22. Outeiro TF, Lindquist S. Yeast cells provide insight into α-synuclein biology and pathobiology. Science 2003; 302:1772-5.
23. True HL, Lindquist SL. A yeast prion provides a mechanism for genetic variation and phenotypic diversity. Nature 2000; 407:477-83.
24. Shorter J, Lindquist S. Prions as adaptive conduits of memory and inheritance. Nat Rev Genet 2005; 6:435-50.

25. Papassotiropoulos A, Wollmer MA, Aguzzi A, Hock C, Nitsch RM, de Quervain DJ. The prion gene is associated with human long-term memory. Hum Mol Genet 2005; 14:2241-6.
26. Krobitsch S, Lindquist S. Aggregation of huntingtin in yeast varies with the length of the polyglutamine expansion and the expression of chaperone proteins. Proc Natl Acad Sci USA 2000; 97:1589-94.
27. Muchowski PJ, Ning K, D'Souza-Schorey C, Fields S. Requirement of an intact microtubule cytoskeleton for aggregation and inclusion body formation by a mutant huntingtin fragment. Proc Natl Acad Sci USA 2002; 99:727-32.
28. Warrick JM, Chan HY, Gray-Board GL, Chai Y, Paulson HL, Bonini NM. Suppression of polyglutamine-mediated neurodegeneration in *Drosophila* by the molecular chaperone HSP70. Nat Genet 1999; 23:425-8.
29. Waelter S, Boeddrich A, Lurz R, Scherzinger E, Lueder G, Lehrach H, Wanker EE. Accumulation of mutant huntingtin fragments in aggresome-like inclusion bodies as a result of insufficient protein degradation. Mol Biol Cell 2001; 12:1393-407.
30. Carmichael J, Chatellier J, Woolfson A, Milstein C, Fersht AR, Rubinsztein DC. Bacterial and yeast chaperones reduce both aggregate formation and cell death in mammalian cell models of Huntington's disease. Proc Natl Acad Sci USA 2000; 97:9701-5.
31. Davies SW, Turmaine M, Cozens BA, DiFiglia M, Sharp AH, Ross CA, Scherzinger E, Wanker EE, Mangiarini L, Bates GP. Formation of neuronal intranuclear inclusions underlies the neurological dysfunction in mice transgenic for the HD mutation. Cell 1997; 90:537-48.
32. Hughes RE, Lo RS, Davis C, Strand AD, Neal CL, Olson JM, Fields S. Altered transcription in yeast expressing expanded polyglutamine. Proc Natl Acad Sci USA 2001; 98:13201-6.
33. Duennwald ML, Jagadish S, Muchowski PJ, Lindquist S. Flanking sequences profoundly alter polyglutamine toxicity in yeast. Proc Natl Acad Sci USA 2006.
34. Masison DC, Maddelein ML, Wickner RB. The prion model for [URE3] of yeast: Spontaneous generation and requirements for propagation. Proc Natl Acad Sci USA 1997; 94:12503-8.
35. Ter-Avanesyan MD, Dagkesamanskaya AR, Kushnirov VV, Smirnov VN. The SUP35 omnipotent suppressor gene is involved in the maintenance of the non-Mendelian determinant [PSI$^+$] in the yeast *Saccharomyces cerevisiae*. Genetics 1994; 137:671-6.
36. Vitrenko YA, Pavon ME, Stone SI, Liebman SW. Propagation of the [PIN+] prion by fragments of Rnq1 fused to GFP. Curr Genet 2007; 51:309-19.
37. Ross ED, Edskes HK, Terry MJ, Wickner RB. Primary sequence independence for prion formation. Proc Natl Acad Sci USA 2005; 102:12825-30.
38. Maddelein ML, Wickner RB. Two prion-inducing regions of Ure2p are nonoverlapping. Mol Cell Biol 1999; 19:4516-24.
39. Perez-Martin J. Chromatin and transcription in *Saccharomyces cerevisiae*. FEMS Microbiol Rev 1999; 23:503-23.
40. Michelitsch MD, Weissman JS. A census of glutamine/asparagine-rich regions: Implications for their conserved function and the prediction of novel prions. Proc Natl Acad Sci USA 2000; 97:11910-5.
41. Winzeler EA, Shoemaker DD, Astromoff A, Liang H, Anderson K, Andre B, Bangham R, Benito R, Boeke JD, Bussey H, Chu AM, Connelly C, Davis K, Dietrich F, Dow SW, El Bakkoury M, Foury F, Friend SH, Gentalen E, Giaever G, Hegemann JH, Jones T, Laub M, Liao H, Liebundguth N, Lockhart DJ, Lucau-Danila A, Lussier M, M'Rabet N, Menard P, Mittmann M, Pai C, Rebischung C, Revuelta JL, Riles L, Roberts CJ, Ross-MacDonald P, Scherens B, Snyder M, Sookhai-Mahadeo S, Storms RK, Veronneau S, Voet M, Volckaert G, Ward TR, Wysocki R, Yen GS, Yu K, Zimmermann K, Philippsen P, Johnston M, Davis RW. Functional characterization of the *S. cerevisiae* genome by gene deletion and parallel analysis. Science 1999; 285:901-6.
42. Spang A, Geissler S, Grein K, Schiebel E. Gamma-Tubulin-like Tub4p of *Saccharomyces cerevisiae* is associated with the spindle pole body substructures that organize microtubules and is required for mitotic spindle formation. J Cell Biol 1996; 134:429-41.
43. Burke D, Dawson D, Stearns T. Methods in yeast genetics: A cold spring harbor laboratory course manual. Cold Spring Harbor, NY: Cold Spring Harbor Laboratory Press, 2000.
44. Sikorski RS, Hieter P. A system of shuttle vectors and yeast host strains designed for efficient manipulation of DNA in *Saccharomyces cerevisiae*. Genetics 1989; 122:19-27.
45. Cormack BP, Bertram G, Egerton M, Gow NA, Falkow S, Brown AJ. Yeast-enhanced green fluorescent protein (yEGFP)a reporter of gene expression in Candida albicans. Microbiology 1997; 143:303-11.
46. An X, Zhang Z, Yang K, Huang M. Cotransport of the heterodimeric small subunit of the *Saccharomyces cerevisiae* ribonucleotide reductase between the nucleus and the cytoplasm. Genetics 2006; 173:63-73.
47. Wanker EE, Scherzinger E, Heiser V, Sittler A, Eickhoff H, Lehrach H. Membrane filter assay for detection of amyloid-like polyglutamine-containing protein aggregates. Methods Enzymol 1999; 309:375-86.
48. Huang M, Zhou Z, Elledge SJ. The DNA replication and damage checkpoint pathways induce transcription by inhibition of the Crt1 repressor. Cell 1998; 94:595-605.
49. Efron B, Tibshirani RJ. An Introduction to the Bootstrap. New York: Chapman and Hall Inc., 1993.
50. Muchowski PJ, Schaffar G, Sittler A, Wanker EE, Hayer-Hartl MK, Hartl FU. Hsp70 and hsp40 chaperones can inhibit self-assembly of polyglutamine proteins into amyloid-like fibrils. Proc Natl Acad Sci USA 2000; 97:7841-6.
51. Campbell BC, Li QX, Culvenor JG, Jakala P, Cappai R, Beyreuther K, Masters CL, McLean CA. Accumulation of insoluble α-synuclein in dementia with Lewy bodies. Neurobiol Dis 2000; 7:192-200.
52. Schaffar G, Breuer P, Boteva R, Behrends C, Tzvetkov N, Strippel N, Sakahira H, Siegers K, Hayer-Hartl M, Hartl FU. Cellular toxicity of polyglutamine expansion proteins: Mechanism of transcription factor deactivation. Mol Cell 2004; 15:95-105.
53. Willingham S, Outeiro TF, DeVit MJ, Lindquist SL, Muchowski PJ. Yeast genes that enhance the toxicity of a mutant huntingtin fragment or α-synuclein. Science 2003; 302:1769-72.
54. Kopito RR. Aggresomes, inclusion bodies and protein aggregation. Trends Cell Biol 2000; 10:524-30.
55. Garcia-Mata R, Gao YS, Sztul E. Hassles with taking out the garbage: Aggravating aggresomes. Traffic 2002; 3:388-96.
56. Taylor JP, Tanaka F, Robitschek J, Sandoval CM, Taye A, Markovic-Plese S, Fischbeck KH. Aggresomes protect cells by enhancing the degradation of toxic polyglutamine-containing protein. Hum Mol Genet 2003; 12:749-57.
57. Johnston JA, Ward CL, Kopito RR. Aggresomes: A cellular response to misfolded proteins. J Cell Biol 1998; 143:1883-98.
58. Fonte V, Kapulkin V, Taft A, Fluet A, Friedman D, Link CD. Interaction of intracellular β amyloid peptide with chaperone proteins. Proc Natl Acad Sci USA 2002; 99:9439-44.
59. Meriin AB, Zhang X, He X, Newnam GP, Chernoff YO, Sherman MY. Huntington toxicity in yeast model depends on polyglutamine aggregation mediated by a prion-like protein Rnq1. J Cell Biol 2002; 157:997-1004.
60. Cao F, Levine JJ, Li SH, Li XJ. Nuclear aggregation of huntingtin is not prevented by deletion of chaperone Hsp104. Biochim Biophys Acta 2001; 1537:158-66.
61. Gokhale KC, Newnam GP, Sherman MY, Chernoff YO. Modulation of prion-dependent polyglutamine aggregation and toxicity by chaperone proteins in the yeast model. J Biol Chem 2005; 280:22809-18.
62. Lin X, Antalffy B, Kang D, Orr HT, Zoghbi HY. Polyglutamine expansion down-regulates specific neuronal genes before pathologic changes in SCA1. Nat Neurosci 2000; 3:157-63.
63. Bhaumik SR, Green MR. Differential requirement of SAGA components for recruitment of TATA-box-binding protein to promoters in vivo. Mol Cell Biol 2002; 22:7365-71.
64. Huisinga KL, Pugh BF. A TATA Binding Protein regulatory network that governs transcription complex assembly. Genome Biol 2007; 8:R46.
65. Perutz MF, Pope BJ, Owen D, Wanker EE, Scherzinger E. Aggregation of proteins with expanded glutamine and alanine repeats of the glutamine-rich and asparagine-rich domains of Sup35 and of the amyloid β-peptide of amyloid plaques. Proc Natl Acad Sci USA 2002; 99:5596-600.
66. Shimohata T, Sato A, Burke JR, Strittmatter WJ, Tsuji S, Onodera O. Expanded polyglutamine stretches form an 'aggresome'. Neurosci Lett 2002; 323:215-8.
67. Ravikumar B, Duden R, Rubinsztein DC. Aggregate-prone proteins with polyglutamine and polyalanine expansions are degraded by autophagy. Hum Mol Genet 2002; 11:1107-17.
68. Derkatch IL, Bradley ME, Zhou P, Chernoff YO, Liebman SW. Genetic and environmental factors affecting the de novo appearance of the [PSI$^+$] prion in *Saccharomyces cerevisiae*. Genetics 1997; 147:507-19.
69. Derkatch IL, Uptain SM, Outeiro TF, Krishnan R, Lindquist SL, Liebman SW. Effects of Q/N-rich, polyQ, and non-polyQ amyloids on the de novo formation of the [PSI$^+$] prion in yeast and aggregation of Sup35 in vitro. Proc Natl Acad Sci USA 2004; 101:12934-9.
70. Yang W, Dunlap JR, Andrews RB, Wetzel R. Aggregated polyglutamine peptides delivered to nuclei are toxic to mammalian cells. Hum Mol Genet 2002; 11:2905-17.
71. Li SH, Cheng AL, Zhou H, Lam S, Rao M, Li H, Li XJ. Interaction of Huntington disease protein with transcriptional activator Sp1. Mol Cell Biol 2002; 22:1277-87.
72. Shimohata T, Onodera O, Tsuji S. Interaction of expanded polyglutamine stretches with nuclear transcription factors leads to aberrant transcriptional regulation in polyglutamine diseases. Neuropathology 2000; 20:326-33.
73. Huang CC, Faber PW, Persichetti F, Mittal V, Vonsattel JP, MacDonald ME, Gusella JF. Amyloid formation by mutant huntingtin: Threshold, progressivity and recruitment of normal polyglutamine proteins. Somat Cell Mol Genet 1998; 24:217-33.
74. Nucifora Jr FC, Sasaki M, Peters MF, Huang H, Cooper JK, Yamada M, Takahashi H, Tsuji S, Troncoso J, Dawson VL, Dawson TM, Ross CA. Interference by huntingtin and atrophin-1 with cbp-mediated transcription leading to cellular toxicity. Science 2001; 291:2423-8.
75. Steffan JS, Kazantsev A, Spasic-Boskovic O, Greenwald M, Zhu YZ, Gohler H, Wanker EE, Bates GP, Housman DE, Thompson LM. The Huntington's disease protein interacts with p53 and CREB-binding protein and represses transcription. Proc Natl Acad Sci USA 2000; 97:6763-8.
76. Krogan NJ, Cagney G, Yu H, Zhong G, Guo X, Ignatchenko A, Li J, Pu S, Datta N, Tikuisis AP, Punna T, Peregrin-Alvarez JM, Shales M, Zhang X, Davey M, Robinson MD, Paccanaro A, Bray JE, Sheung A, Beattie B, Richards DP, Canadien V, Lalev A, Mena F, Wong P, Starostine A, Canete MM, Vlasblom J, Wu S, Orsi C, Collins SR, Chandran S, Haw R, Rilstone JJ, Gandi K, Thompson NJ, Musso G, St Onge P, Ghanny S, Lam MH, Butland G, Altaf-Ul AM, Kanaya S, Shilatifard A, O'Shea E, Weissman JS, Ingles CJ, Hughes TR, Parkinson J, Gerstein M, Wodak SJ, Emili A, Greenblatt JF. Global landscape of protein complexes in the yeast *Saccharomyces cerevisiae*. Nature 2006; 440:637-43.
77. Gavin AC, Aloy P, Grandi P, Krause R, Boesche M, Marzioch M, Rau C, Jensen LJ, Bastuck S, Dumpelfeld B, Edelmann A, Heurtier MA, Hoffman V, Hoefert C, Klein K, Hudak M, Michon AM, Schelder M, Schirle M, Remor M, Rudi T, Hooper S, Bauer A, Bouwmeester T, Casari G, Drewes G, Neubauer G, Rick JM, Kuster B, Bork P, Russell RB, Superti-Furga G. Proteome survey reveals modularity of the yeast cell machinery. Nature 2006; 440:631-6.